ISSN 1062-8738, Bulletin of the Russian Academy of Sciences: Physics, 2020, Vol. 84, No. 2, pp. 220–224. © Allerton Press, Inc., 2020.
Russian Text © The Author(s), 2020, published in Izvestiya Rossiiskoi Akademii Nauk, Seriya Fizicheskaya, 2020, Vol. 84, No. 2, pp. 278–283.

Using Spaced Combined Receiving Modules to Study the Scalar–Vector Characteristics of an Acoustic Field

E. V. Medvedeva[a, *], B. I. Goncharenko[a], and A. S. Shurup[a, b, c]

[a] *Moscow State University, Moscow, 119991 Russia*
[b] *Shirshov Institute of Oceanology, Russian Academy of Sciences, Moscow, 117218 Russia*
[c] *Schmidt Institute of Physics of the Earth, Russian Academy of Sciences, Moscow, 123995 Russia*
**e-mail: medvedeva.ev15@physics.msu.ru*

Received August 26, 2019; revised September 13, 2019; accepted October 28, 2019

Abstract—Field experiments to measure the scalar–vector structure of an acoustic field at a Moscow State University hydroacoustic test site with an ice cover are analyzed. The anisotropy of the noise field in the water is estimated. Noise cross-correlation functions are constructed using the directional characteristics of two spaced combined receiving modules.

DOI: 10.3103/S1062873820020240

INTRODUCTION

An important way of studying large areas of ocean is passive acoustic tomography, which is based on a theoretically substantiated procedure for estimating Green's function for two spaced points via the cross correlation of diffuse noise fields specified at those points [1]. For passive monitoring, the scheme is two hydrophones spaced arbitrarily at a certain distance in the area water where isotropic acoustic noise is observed; part of the noise propagates through both hydrophones in turn and forms the desired signal. This situation is equivalent to a scheme in which one hydrophone transmits a signal and the second one receives it. Noises coming from other directions are considered interference. The main factor that determines the efficiency of using passive tomography is the period of noise signal accumulation [1]. In our opinion, a promising area in the development of passive acoustic tomography is the use of combined receiving modules that can record both the scalar and vector characteristics of acoustic fields at one point in space [2]. This approach allows us to obtain a much larger volume of information on the structure of a wave field in a period comparable to the one possible when using solitary pressure receivers. Theoretical estimates show [3] that using combined receiving modules in passive tomography considerably reduces the period of noise signal accumulation required for a reliable estimate of Green's function.

The aim of this work was to analyze experimental data [4] obtained at a Moscow State University hydroacoustic test site in the winter of 2019 by making measurements in the water of an ice-covered Klyaz'ma Reservoir. To perform our experiments, we selected an extensive horizontal area of a water layer approximately 8 m deep and covered by ice 40–50 cm thick at some distance from the shore. Two combined receiving modules (CRM 1 and CRM 2) were spaced on the bottom, first at 40 m and then at 90 m. They were used to measure simultaneously sound pressure and three mutually orthogonal components of the noise field's rate of vibration. The orientation of the receiving modules' X channels was known: $\varphi_1 = 250°$ NW and $\varphi_2 = 257°$ NW, relative to true north.

PRIMARY CORRELATION PROCESSING

The experimental data were processed to synchronize the signals arriving from both receiving modules to a set of analog-to-digital converters. To accomplish this, an FM signal was transmitted to additional channels of both converters in real time from the same radio station as the acoustic measurements were being recorded. The relative time delays of cross-correlation function (1) were calculated for each sample of the signal recorded from the two different converters. The signal from CRM 2 was then interpolated to a new time axis with allowance for the delays, synchronizing the signals from the radio channels with accuracy up to the point of reference. The signals from the channels of CRM 2 and 3 were processed using this algorithm. Synchronization allowed us to move on to correlation analysis of the noise fields in the water to derive the desired signal propagating between the receivers against the background noise.

The cross-correlation function was calculated for noise fields $p(\vec{r}_1, t)$ and $p(\vec{r}_2, t)$, recorded at two points

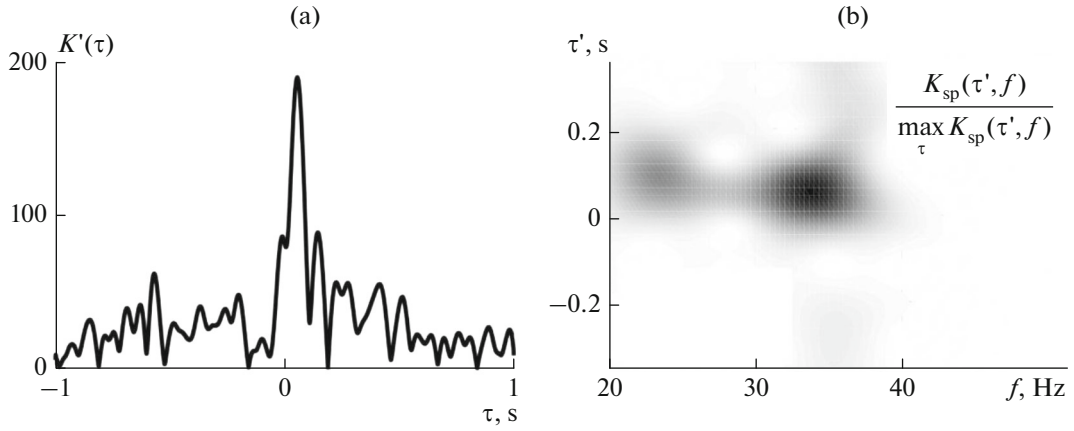

Fig. 1. (a) Envelope of the derivative of the cross-correlation function of whitened noise signals received on a pair of hydrophones spaced at 40 m; (b) normalized spectrogram of the derivative of the correlation function for 40 m.

$\vec{r}_1$ and $\vec{r}_2$ (where $\vec{r} = \{x, y, z\}$ is the radius vector), corresponding to the positions of receivers 1 and 2, respectively:

$$K(\tau) = \frac{1}{T}\int_0^T p(\vec{r}_1, t)\, p(\vec{r}_2, t - \tau)dt, \qquad (1)$$

where T is the period of noise accumulation. Function $K(\tau)$ is expected to have two symmetrical peaks. The peaks in the positive part of time scale τ correspond to the recording of the signals propagating from CRM 1 to CRM 2, while those in the negative part match the signals traveling to the opposite side. Time delays τ corresponding to the maxima of $K(\tau)$ are determined by the time required for the signal to propagate between the hydrophones. For a more accurate estimate of the length of signal propagation, we subsequently analyze the envelope of derivative correlation function (1) by time delay τ [5].

Measurements made with the ice cover produced signal recordings 45 min long, obtained using two CRMs spaced at 40 and 90 m. After whitening [5], they approximated a stationary noise that was close to white, the spectral components of which were distributed uniformly across the range of frequencies. All recordings were broken down into segments of 120 s, and a cross-correlation function was obtained for each one in the frequency band of 20–45 Hz using formula (1). Summing and normalizing to the maximum value, a single correlation peak was observed for both distances around the zero lag (Fig. 1a). We could identify no second peak symmetrical to the first one.

To analyze our results, we calculated the spectrograms of correlation functions $K(\tau)$:

$$K_{sp}(\tau', f) = \int_{-\infty}^{+\infty} K(\tau) h(\tau - \tau') \exp(-i2\pi f\tau)dt, \qquad (2)$$

where $h(\tau)$ is a rectangular window function.

The spectrogram constructed using short time Fourier transform (2) (Fig. 1b) shows that most of the energy of the signal recorded by the two CRMs was focused in the range of 30–40 Hz, which could correspond to the frequency of propagation of one of the lowest acoustic modes. It was shown in [6] that the main contribution to the formation of the noise correlation function comes from the stationary phase point corresponding to the local minimum in the group velocity of the considered mode. According to our estimates, however, the critical frequency of the first normal wave was only 80–100 Hz under the experimental conditions.

A numerical study showed that when there is an intermediary layer with a speed of sound around 100–300 m/s at the bottom of a water area, a wave can partly localize in this low-speed layer, the group velocity of which has a minimum of around 35 Hz. Such a low-velocity layer of sediments is known to exist in the waters of Klyaz'ma Reservoir. This is explained by a high content of methane bubbles [7] and considerably reduces the speed of sound. Figure 2a shows the profile of the speed of sound versus depth for a three-layer waveguide model with an ice cover, where $h = 0$–0.5 m corresponds to $c = 2200$ m/s (ice); $h = 0.5$–7 m, to $c = 1450$ m/s (water); $h = 7$–8.3 m to $c = 100$ m/s (a gas-saturated layer); and $h = 8.3$ m and deeper, to $c = 1800$ m/s (the bottom, in the form of a liquid half-space). The ratio of the densities of the bottom and the water layer is $\rho_b/\rho_l = 2.1$. The results from numerical modeling for the above parameters of the waveguide yielded an estimate of the group velocity of a wave whose minimum falls within frequencies of 35–40 Hz. Note that such a wave had never been observed experimentally before.

Nothing needs to be radiated when using passive means of study, which is a clear advantage of such techniques. In our case, this allowed us begin studying a low-frequency hydroacoustic field, which is a complex problem in the active regime due to technical

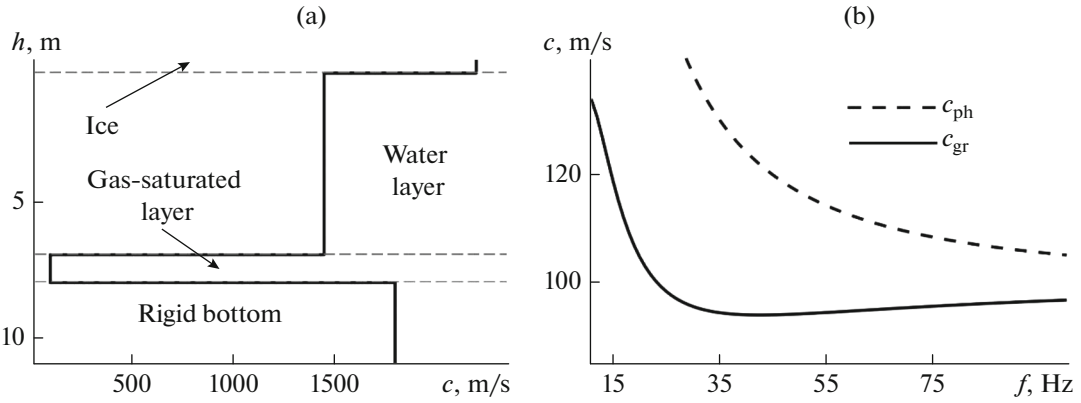

Fig. 2. (a) Profile of speed of sound c in the water of Klyaz'ma Reservoir with respect to depth h; dependence of phase c_{ph} and group c_{gr} velocities on frequency f; (b) results from numerical modeling for the specified profile of the speed of sound.

restrictions on the possibility of radiating low-frequency sound.

The correlation function obtained by processing noise (Fig. 1) contained no peaks symmetrical to a zero lag, which requires separate consideration. This could be due to the pronounced anisotropy of the noise field (i.e., there being a preferential direction from which the main energy of a recorded noise signal arrives).

STUDYING THE SPATIAL ANISOTROPY OF A NOISE FIELD

To study the reasons for the emergence of a single peak relative to a zero lag instead of two symmetrical ones, we estimated the distribution of intensity in a recorded signal with respect to the angle of the direction [8] in the range of 20–45 Hz for both CRMs. The selected band of frequencies was divided into $N = 100$ different discrete components f_i, for each of which we calculated azimuth angle φ_i. Intensity was determined as the sum of the modules of the components in the vector of the flow of acoustic power, averaged with respect to the recorded time:

$$\tan\varphi_i = \frac{W_{Ry,i}}{W_{Rx,i}}, \quad I(f_i,\varphi_i) = \sqrt{W_{Rx,i}^2 + W_{Ry,i}^2}, \qquad (3)$$

where $W_{Rx,i}$ and $W_{Ry,i}$ are the projections of the flow of acoustic power for each component i in directions x and y.

We then divided the range of angles from 0° to 360° into $M = 100$ sectors with widths $\Delta\varphi_0 = 3.6°$. This determined the angular resolution for specified number of sectors M. Next, we plotted a histogram for total intensities $I(\varphi_n)$ of the signals falling into each sector:

$$I(\varphi_n) = \sum_{i=1}^{N} I(f_i, [n-1]\Delta\varphi_0 \le \varphi_i < n\Delta\varphi_0), \qquad (4)$$

where $\varphi_n = \Delta\varphi_0\left(n + \frac{1}{2}\right)$, $n = 1, 2, ..., M$. Figures 3a, 3b illustrate the result from plotting $I(\varphi_n)$ for the above processing parameters. It is seen that the noise field has strongly pronounced anisotropy. Peaks of intensity are recorded at ~340° for CRM 1 and ~65° for CRM 2 with an approximately 3.5° accuracy of determining the angle. Based on the estimated direction of the noise signal's arrival, and allowing for the known configuration of the distribution of vector receiver channels, we suggest that the CRM sound receivers also recorded a wave propagating in a direction different from the straight line along which the receiving modules were positioned. This explains why the correlation function has only one peak. This intensity of the wave is much greater than that of the noise coming from other directions, so no symmetrical peaks of the cross-correlation function are observed.

For self-corroboration, we also plotted the time dependences of the angles of arrival using algorithm (3). On average, the angles of arrival were 69° ± 3.5° and 341° ± 2.8° for CRM 1 and CRM 2, respectively; this coincides with the direction marked in the histogram of intensities and confirms our assumption there was pronounced spatial anisotropy of the noise field in the body of water. This feature of the recorded noise field must be considered separately when constructing noise correlations.

CONSTRUCTING THE NOISE CROSS-CORRELATION FUNCTION USING A CARDIOID

Since the interference's direction of arrival is known and we have information on the mutual orientation of the receiving modules' X channels, we can construct cross-correlation functions that allow for the anisotropy of noises. The correlation processing algorithm used in this case was similar to (1), the standard procedure. In order to determine the directions of noise signal propagation, which were of greatest interest, we also shaped the cardioid characteristics of directivity on each CRM:

$$U = P + \rho c\left(V_x \cos\varphi + V_y \sin\varphi\right). \qquad (5)$$

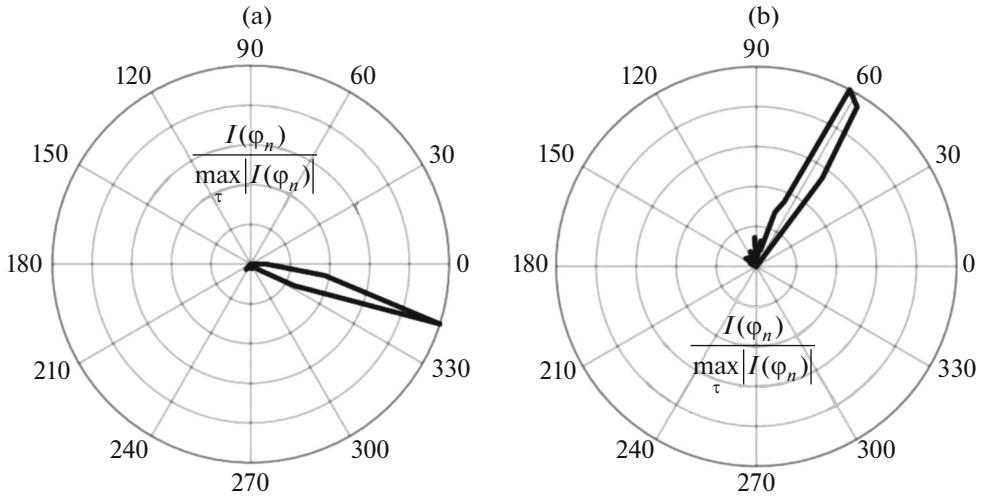

Fig. 3. Angular distribution of the intensity of noise characterizing its spatial anisotropy for (a) CRM 1 and (b) CRM 2 in the 20–45 Hz band of frequencies over 45 min of observations.

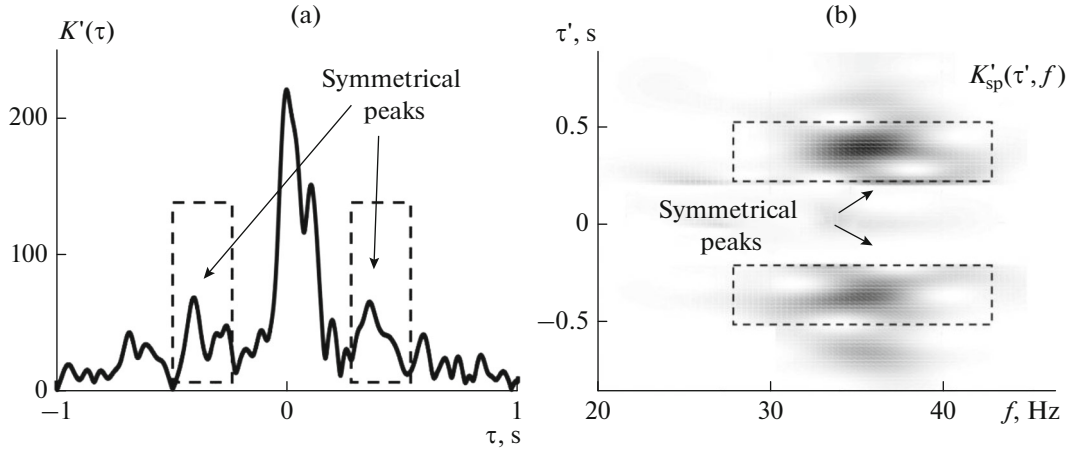

Fig. 4. (a) Envelope of the derivative of the cross-correlation function for the angles characterizing the directions to cardioid maxima $\varphi_1 = \pi$ and $\varphi_2 = 0$; (b) normalized spectrogram of the derivative of the cross-correlation directional function for a pair of hydrophones spaced at 40 m with $\varphi_1 = \pi$ and $\varphi_2 = 0$.

An alternative approach is to form such a cardioid in which the effect of interference from a specified direction is removed by turning the cardioid's minimum in the direction of intense interference. For formed functions U (5), we plotted the cross-correlation functions referred to below as directional correlations. The directions of the cardioid maxima were selected as azimuth angles in two ways. In one (Fig. 4a), angles $\varphi_1 = \pi$ and $\varphi_2 = 0$ were designated azimuth angle φ. As a result, the characteristics of the two CRMs' directivity were co-oriented in directions opposite to each other. In the second, the azimuth angles were selected as $\varphi_1 = \varphi(t) + 180°$ and $\varphi_2 = \varphi(t) + 180°$, where $\varphi(t)$ are the angles of arrival as estimates of the direction to the identified noise interference obtained earlier. We thus attempted to offset interference in the considered band of frequencies.

For the directional correlations in Fig. 4a, we can see symmetrical correlation maxima standing out among the noise, despite interference near the zero lag that was not removed completely. In the 20–45 Hz range of frequencies, these peaks correspond to the wave localized in the bottom layer, as was noted earlier. The shift of the peaks relative to zero is about 0.4 s, allowing us to estimate the speed of a wave traveling along the straight line connecting the two CRMs. Our estimate yields a speed of 100 m/s, which is consistent with our assumption about the possible formation of a low-velocity sound wave in the gas-saturated mud of Klyaz'ma Reservoir's bottom layer.

Formula (2) was also used to construct the spectrograms of the derivative correlation functions for the two different ways of denoting angles φ, in analogy to the preliminary calculations. For greater clarity, a filter was applied to the central band in the time range of −0.2 to 0.2 s, reducing the intensity by a factor of 20 and allowing us to distinguish areas of the concentration of noise propagating between the CRMs. Figure 4b shows they were localized in the 30–40 Hz range of frequencies, as the main interference suppressed by the filter.

A wave propagating at a speed of sound considerably lower than the one in the water layer was thus recorded in the gas-saturated intermediate layer of mud using combined sound receivers separated in space. Signals at frequencies around 35 Hz were not analyzed in experiments performed earlier in the waters of Klyaz'ma Reservoir [9].

The use of a cardioid in correlation processing allowed us to identify symmetrical peaks against the background of intense anisotropic interference. The described procedure for constructing a directional cross-correlation function is promising for analyzing different ranges of frequencies with propagating waves that carry information on different characteristics of a waveguide (i.e., those of a water layer in the high-frequency range and the parameters of a bottom in the low-frequency range).

CONCLUSIONS

Data obtained during field measurements plus the processing algorithms executed numerically and tested in this work form the basis for developing means of passive tomography for a shallow sea using the scalar–vector characteristics of the solund field. A potential area of future development is the correlation processing of noise in order to form a cardioid at each combined receiving module in different ranges frequencies, along with creating a passive monitoring scheme that considers the anisotropy of the noise field. According to theoretical estimates and preliminary experimental results [1, 4], the period of noise accumulation required for a reliable estimate of the length of signal propagation between receiving stations can be reduced substantially in this case, compared to using single pressure receivers.

FUNDING

This work was supported by the Russian Foundation for Basic Research, project nos. 18-05-70034 and 18-05-00737.

REFERENCES

1. Burov, V.A., Sergeev, S.N., and Shurup, A.S., *Acoust. Phys.*, 2008, vol. 54, no. 1, p. 42.
2. Gordienko, V.A., *Vektorno-fazovye metody v akustike* (Vector-Phase Methods in Acoustics), Moscow: Fizmatlit, 2007.
3. Gordienko, V.A., Goncharenko, B.I., and Ilyushin, Ya.A., *Acoust. Phys.*, 1993, vol. 39, no. 3, p. 455.
4. Medvedeva, E.V., *Trudy XXVI Mezhdunarodnoi konferentsii "Lomonosov-2019"* (Proc. XXVI Int. Conf. "Lomonosov-2019"), Moscow, 2019, p. 22.
5. Bensen, G.D., Ritzwoller, M.H., Barmin, M.P., et al., *Geophys. J. Int.*, 2007, vol. 169, p. 1239.
6. Burov, V.A., Grinyuk, F.V., Kravchenko, V.N., Mukhanov, P.Yu., Sergeev, S.N., and Shurup, A.S., *Acoust. Phys.*, 2014, vol. 60, no. 6, p. 647.
7. Rozhin, F.V. and Tonakanov, O.S., *Obshchaya gidroakustika* (General Hydroacoustics), Moscow: Mosk. Gos. Univ., 1988.
8. Gordienko, V.A., Gordienko, T.V., Krasnopistzev, N.V., and Nekrasov, V.N., *Moscow Univ. Phys. Bull.*, 2014, vol. 69, no. 2, p. 105.
9. Goncharenko, B.I., Zakharov, L.N., and Ivanov, V.E., *Akust. Zh.*, 1979, vol. 25, no. 4, p. 507.

Translated by L. Mukhortova